Multiple return analysis for noncoherent pulse compression of periodic coded waveforms

Itzik Cohen[1], Nadav Levanon[1], Avi Zadok[2]

1 – Department of Electrical Engineering - Systems, Tel Aviv University,
Chaim Levanon Street, 6997801, Tel Aviv, Israel
2 – Faculty of Engineering and Institute for Nano-Technology and Advanced Materials,
Bar-Ilan University, Ramat-Gan 5290002, Israel

Abstract **Recently proposed direct-detection laser range finders transmit low power, periodic, unipolar (ON-OFF) coded signal, instead of the commonly used strong narrow single pulse. The combination of non-coherent pulse compression (NCPC) and appropriate binary sequences produces a sidelobe-free periodic delay response. The continuous wave (CW) nature of the signal results in overlaps between returns from multiple targets. When envelope detected, the overlaps can create intermodulation that may hurt the sidelobe-free range response. The paper studies the effect of different sequence types and different envelope detector response profiles and suggests measures to mitigate the influence of multiple targets by calibration of envelope detector.**

I. Introduction

Pulse compression is a well-established radar technique that creates a virtual narrow strong pulse out of a weak long pulse [1], [2]. Pulse compression is achieved by modulating the transmitted long pulse and correlating its received reflection with a reference modulated-pulse stored in the receiver. Noncoherent pulse compression (NCPC) studied recently [3]–[8], employs on-off keying (OOK) modulation. NCPC is of interest to direct-detection laser radar (LIDAR), and to simple radars that utilize noncoherent microwave power source (such as magnetron transmitters) [9]–[13].

Previous researches [14], [15] include extensive analysis of the performances of NCPC in the presence of noise. However, research to date did not yet address the performances of NCPC when returns from multiple targets overlap. This is likely to happen when continuous wave (CW) waveforms are used. Since the returns are processed by a noncoherent processor, following an envelope detector, the process is non-linear, and overlaps can cause intermodulation. The nature and characteristics of the intermodulation effect depend on the specific setup of the targets (number of returns, relative delays, and relative amplitudes between the returns). The manifestation of intermodulation effects is also waveform dependent, where for some waveforms it would translate as ghost targets, and for some others it would practically introduce a noise-like signal at all delay bins. The envelope detector's profile (linear, square, logarithmic, etc.) also has influence on the extent and magnitude of sidelobes.

Fig. 1 illustrates these phenomena, using two targets as suggested in [7]. The targets are at delay bins number 100 and 200, and the returned amplitude of the second target is half the amplitude relative to the return of the first target. The two graphs in this figure differ by the type of waveform used in each one. In Fig. 1 (a), a length 1019 periodic Legendre code is used, and the resulted correlation output shows two peaks at the correct delays with noise-like sidelobes. For Fig. 1 (b), a length 1023 periodic m-sequence is used, and the resulted correlation output shows two peaks matching the correct delays of the target returns, with an additional ghost peak at delay bin number 706.

This paper presents an analysis of this intermodulation effect of multiple returns with additive noise, for the specific case of periodic NCPC. The paper shows that this intermodulation simply does not exist when using squared-law envelope detector, but will appear if the detector deviates from squared-law profile, even slightly. The paper also proposes a calibration method of the squared-law detector, using unique patterns caused by intermodulation.

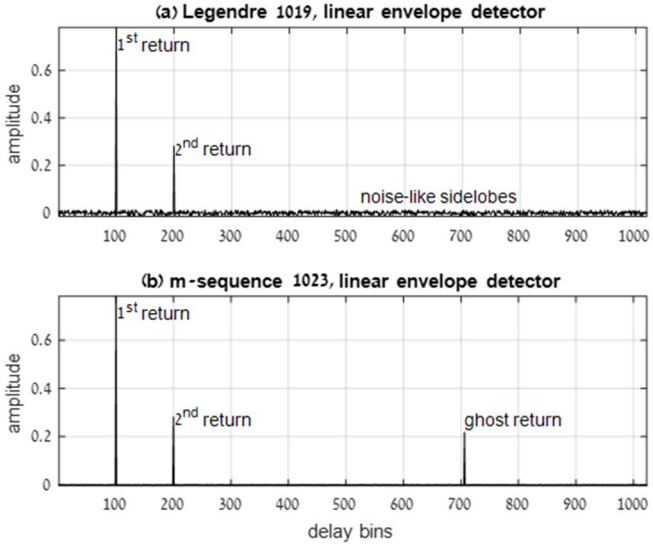

Fig. 1. Processed returns of two targets using linear envelope detector, (a) - length 1019 Legendre code, (b) - length 1023 m-sequence.

II. Analysis of Multiple Returns in the Presence of Noise

A. Signal model and asymptotic statistics

The transmitted signal is a periodic unipolar binary (on-off) sequence c_n, where for the scope of this paper, the sequence c_n is a perfect-periodic correlation (PPC) sequence [7] (for

example, m-sequence or Legendre). The period of the sequence will be noted as N.

The received signal is a superposition of returns from K targets, each with its own amplitude, phase, and time delay (α_k, $\varphi_{k,n}$ and d_k, respectively), with additive white complex-normal noise w_n:

$$s_n = \sum_{k=1}^{K} \alpha_k e^{j\varphi_{k,n}} c_{n-d_k} + \mathrm{w}_n. \tag{1}$$

The target amplitude and delay parameters (α_k and d_k) are non-negative fixed values, the phase has uniform distribution in the range of $[0,2\pi]$, and as the source is non-coherent, the phase samples are statistically independent.

The received signal is processed by envelope detector, followed by pulse compression filter, with a reference signal $\tilde{c}_n$, matched to the unipolar sequence c_n such that the correlation is perfect-periodic. In the specific cases of m-sequence and Legendre codes, the reference signal $\tilde{c}_n$ is simply the bi-polar version of c_n ($\tilde{c}_n = 2 \cdot c_n - 1$) [7].

The response of the envelope detector is:

$$r_n = f(|s_n|), \tag{2}$$

where $|\cdot|$ denotes element-wise absolute value of the argument, and $f(\cdot)$ is some monotonic amplitude response. Common envelope detector profiles are linear, square-law and logarithmic envelope detectors:

$$\begin{aligned} r_n^{(1)} &= |s_n| \\ r_n^{(2)} &= |s_n|^2 \\ r_n^{(log)} &= log(|s_n|). \end{aligned} \tag{3}$$

As mentioned above, the envelope-detected signal r_n is fed to the pulse compression filter, where P periods of the signal are convolved with the reference signal:

$$y_n = r_n \otimes \tilde{c}_n = \sum_{l=0}^{N\cdot P-1} r_{n+l} \cdot \tilde{c}_l. \tag{4}$$

Note the difference from classic pulse compression, where the matched filter is operating on the received signal s_n, and the response is a superposition of responses to each element in (1) separately [1]. However, for NCPC, as the envelope detector is not linear, such superposition does not apply and the different signal and noise elements would get entangled.

To show the asymptotical behavior of the output signal, the normalized output signal $\tilde{y}_n$ is defined:

$$\tilde{y}_n = \frac{y_n}{P} = \frac{1}{P} \sum_{l=0}^{N\cdot P-1} r_{n+l} \cdot \tilde{c}_l. \tag{5}$$

Assuming that the total number of integrated code elements (number of bits) is high enough ($N \cdot P \gg 1$), using the central limit theorem (CLT), it can be shown that $\tilde{y}_n$ has normal distribution with mean $\overline{\tilde{y}_n} = \mu_{y,n}$ and variance $var\{\tilde{y}_n\} = \sigma_{y,n}^2$. This assumption is valid when the integration time is of several long periods of the sequence, and this is indeed the case for the experimental results presented in [9], [12], [13], [15].

The mean of $\tilde{y}_n$ is:

$$\begin{aligned} \mu_{y,n} &= \overline{\left(\frac{1}{P} \sum_{l=0}^{N\cdot P-1} r_{n+l} \cdot \tilde{c}_l\right)} \\ &= \sum_{l=0}^{N-1} \mu_{r,n+l} \cdot \tilde{c}_l, \end{aligned} \tag{6}$$

and the variance of $\tilde{y}_n$ is:

$$\begin{aligned} \sigma_{y,n}^2 = \sum_{l_1=0}^{N-1} \sum_{l_2=0}^{N-1} M_{r,n+l_1,n+l_2} \cdot \tilde{c}_{l_1} \cdot \tilde{c}_{l_2} \\ -\mu_{y,n}^2, \end{aligned} \tag{7}$$

where $\mu_{r,n}$ and M_{r,n_1,n_2} are the mean and second moment of r_n:

$$\begin{aligned} \mu_{r,n} &= \overline{r_n} \\ M_{r,n_1,n_2} &= \overline{r_{n_1} r_{n_2}}, \end{aligned} \tag{8}$$

Now, after formalizing the signal model, the following sub-sections will present the effect of specific envelope detector profiles and examining the resulted signal by its statistical properties.

B. Linear envelope detector

The response of linear envelope detector is:

$$r_n^{(1)} = |s_n| = \left| \sum_{k=1}^{K} \alpha_k e^{j\varphi_{k,n}} c_{n-d_k} + \mathrm{w}_n \right|, \tag{9}$$

which can be expressed as:

$$r_n^{(1)} = \sqrt{\begin{aligned} &\mathrm{w}_n^2 + \sum_{k=1}^{K} \left(\alpha_k^2 c_{n-d_k}\right) \\ &+ \sum_{k=1}^{K} \left(2\alpha_k c_{n-d_k} w_n \cdot cos\varphi_{k,n}\right) \\ &+ \sum_{\substack{k_1=1 \\ k_2=1 \\ k_1 \neq k_2}}^{K} \begin{pmatrix} \alpha_{k_1}\alpha_{k_2} c_{n-d_{k_1}} c_{n-d_{k_2}} \\ \cdot cos\left(\varphi_{k_1,n} - \varphi_{k_2,n}\right) \end{pmatrix}. \end{aligned}} \tag{10}$$

Calculating the statistics of r_n is relatively cumbersome, so for the scope of this short paper, a simplified problem of only $K = 2$ targets and no additive noise ($w_n = 0$) is discussed in this sub-section. In this case, (10) is simplified to:

$$r_n^{(1)} = \sqrt{\begin{aligned} &\alpha_1^2 c_{n-d_1} + \alpha_2^2 c_{n-d_2} \\ &+2\alpha_1\alpha_2 c_{n-d_1} c_{n-d_2} \\ &\cdot cos\left(\varphi_{1,n} - \varphi_{2,n}\right). \end{aligned}} \tag{11}$$

Using the following integral:

$$\int_0^{2\pi} \sqrt{c + cos\varphi}\, d\varphi = 4\sqrt{c+1} \cdot E\left(\frac{2}{c+1}\right), \tag{12}$$

where $E(\cdot)$ is the complete elliptic integral of the second kind [16], the mean value of $r_n^{(1)}$ is:

$$\begin{aligned} \mu_{r^{(1)},n} &= \overline{r_n^{(1)}} \\ &= \frac{1}{(2\pi)^2} \iint_0^{2\pi} \sqrt{u + v\, cos(\varphi_1 - \varphi_2)} d\varphi_1 d\varphi_2 \\ &= \frac{2}{\pi}\sqrt{u+v}\, E\left(\frac{2v}{u+v}\right), \end{aligned} \tag{13}$$

where $u = \alpha_1^2 c_{n-d_1} + \alpha_2^2 c_{n-d_2}$
and $v = 2\alpha_1\alpha_2 c_{n-d_1} c_{n-d_2}$.

To interpret this result, remember that the amplitudes α_i are fixed non-negative values, and c_i are the uni-polar binary values of the sequence, which serves as indicator terms. Note that in (13), there are terms with product of different c_i values. These product terms are the source of the intermodulation effect of the two returns.

As a toy example, this case of two returns under linear envelope detector is examined using two different sequences: a) length 7 m-sequence, and b) length 11 Legendre. For the simplicity of this example, amplitude values will be set as $\alpha_1 = \alpha_2 = 1$, and delay values are $d_1 = 0$, $d_2 = 1$.

For length 7 m-sequence, the sequence and reference code are:

$$\begin{aligned} c_n &= [\ 0,\ \ 1,\ \ 1,\ \ 1,\ \ 0,\ \ 0,\ \ 1] \\ \tilde{c}_n &= [-1,\ \ 1,\ \ 1,\ \ 1,-1,-1,\ \ 1]. \end{aligned} \tag{14}$$

The expected values of post-envelope detection samples are:

$$\mu_{r^{(1)},n} = [\,\gamma_2,\ \gamma_1,\ \gamma_{12},\ \gamma_{12},\ \gamma_2,\ 0,\ \gamma_1], \tag{15}$$

where γ_1 represents samples where only return #1 exist (as $c_{n-0} = 1$), and in a similar manner, γ_2 represents samples where only return #2 exists, and γ_{12} represents samples where both exists. The values of γ_i are derived from (13):

$$\begin{aligned} \gamma_1 &= \alpha_1 = 1 \\ \gamma_2 &= \alpha_2 = 1 \\ \gamma_{12} &= \frac{2}{\pi}(\alpha_1 + \alpha_2)\, E\left(\frac{2\alpha_1\alpha_2}{(\alpha_1+\alpha_2)^2}\right) = \frac{4}{\pi}. \end{aligned} \tag{16}$$

The mean value of post-matched filter sequence is calculated directly using (6):

$$\mu_{y,n} = \left[\frac{8}{\pi},\ \frac{8}{\pi},\ 0,\ \ 0,\ 0,\ 4-\frac{8}{\pi},\ 0\right]. \tag{17}$$

Repeating the calculations for length 11 Legendre code, the sequence and reference code are:

$$\begin{aligned} c_n &= [1,\ 0,\ 1,\ \ 0,\ \ 0,\ \ 0,\ 1,\ \ 1,\ 1,\ \ 0,\ 1], \\ \tilde{c}_n &= [1,-1,\ 1,-1,-1,-1,\ 1,\ \ 1,\ 1,-1,\ 1], \end{aligned} \tag{18}$$

the expected values of $r_n^{(1)}$ are:

$$\mu_{r^{(1)},n} = [\gamma_{12},\gamma_2,\gamma_1,\gamma_2,0,0,\gamma_1,\gamma_{12},\gamma_{12},\gamma_2,\gamma_1] \tag{19}$$

and the mean output sequence is:

$$\mu_{y,n} = \left[\frac{12}{\pi},\frac{12}{\pi},\beta,\beta,\beta,-\beta,\beta,\beta,-\beta,-\beta,\beta\right], \tag{20}$$

where $\beta = 2 - \frac{4}{\pi}$.

Note the different behavior of responses between m-sequence and Legendre, where for both types of codes there are two peaks at $n = 0$ and $n = 1$ matching the correct delay of the returns (d_1 and d_2), also, the amplitude of the peaks is $\frac{2}{\pi}$ times the number of '1's for each code (4 '1's for the m-sequence, and 6 '1's for the Legendre). However, the m-sequence response shows one additional "ghost" sidelobe and zeros for all other delays, where the Legendre response shows sidelobes along all delay bins. The reason for this behavior is due to a property of m-sequence where a modulo-2 sum (bitwise XOR) of an m-sequence with another phase of the same sequence yields a third phase of the sequence [17]. This property is not valid for Legendre sequences, therefore the mixing of c_1 and c_2 causes pseudo-random sidelobes (in this example, the pseudo-noise has 2 unique values, but this is not always the case).

C. *Square-law envelope detector*

As the previous sub-section showed, if the output of the envelope detection involves mixed terms of different code elements, the resulted output signal of multiple returns would get intermodulated, causing some "ghost" or noise-like sidelobes. This sub-section shows that with square-law detector there is no such intermodulation, as the resulted expressions for the expected post-detection signal has no mixed terms.

The response of square-law envelope detector:

$$r_n^{(2)} = |s_n|^2 = \left|\sum_{k=1}^{K} \alpha_k e^{j\varphi_{k,n}} c_{n-d_k} + \mathrm{w}_n\right|^2, \tag{21}$$

which can be rewritten as:

$$\begin{aligned} r_n^{(2)} = \mathrm{w}_n^2 &+ \sum_{k=1}^{K}\left(\alpha_k^2 c_{n-d_k}\right) \\ &+ \sum_{k=1}^{K}\left(2\alpha_k c_{n-d_k} w_n \cdot cos\varphi_{k,n}\right) \\ &+ \sum_{\substack{k_1=1 \\ k_2=1 \\ k_1\neq k_2}}^{K} \left(\begin{matrix}\alpha_{k_1}\alpha_{k_2} c_{n-d_{k_1}} c_{n-d_{k_2}} \\ \cdot cos\left(\varphi_{k_1,n} - \varphi_{k_2,n}\right)\end{matrix}\right). \end{aligned} \tag{22}$$

Using the fact that integrating over a full period of a cosine is zero, the mean value of $r_n^{(2)}$ becomes:

$$\mu_{r^{(2)},n} = \overline{r_n^{(2)}} = \sigma_w^2 + \sum_{k=1}^{K}\left(\alpha_k^2 c_{n-d_k}\right), \tag{23}$$

where σ_w^2 is the variance of the additive white noise w_n. This expression shows that square-law envelope detector, on average, simply sums up the power of each return, according to the value of the binary indicator c_i. Note that each element in this sum is dependent on only one source, as the integration zeroed all the cross terms.

Combining (23) and (6) yields the expected output signal:

$$\begin{aligned} \mu_{y,n} &= \sum_{l=0}^{N-1}\left(\left(\sigma_w^2 + \sum_{k=1}^{K}\left(\alpha_k^2 c_{n+l-d_k}\right)\right)\cdot \tilde{c}_l\right) \\ &= \sigma_w^2 \sum_{l=0}^{N-1}\tilde{c}_l + \sum_{k=1}^{K}\alpha_k^2 \sum_{l=0}^{N-1} c_{n+l-d_k}\cdot\tilde{c}_l \end{aligned} \tag{24}$$

This expression can be simplified using two properties of the specific sequences in the scope of this paper, where both m-sequence and Legendre a) have perfect periodic cross correlation between the transmitted uni-polar sequence c_n and the bi-polar reference code $\tilde{c}_n$, b) the number of '1' in a period of the sequence is larger by one than the number of '0's. Using these properties, (24) becomes:

$$\mu_{y,n} = \sigma_w^2 + \frac{N+1}{2}\sum_{k=1}^{K}\alpha_k^2\,\delta_{n-d_k}. \tag{25}$$

This expression shows that the resulted output signal is in fact a simple superposition of the input elements, with an impulse matching each return, proportional to the return's received power, at the appropriate delay, with additive noise floor.

D. Small deviation from square-law envelope detector

The previous sub-section showed that while square-law envelope detector is used in NCPC receiver, no intermodulation occurs between multiple returns or between returned signal and noise. However, several aspects should be considered:

a) Practical response of square-law detector might slightly deviate from squared profile.
b) Envelope detectors have limited dynamic range, where beyond it, the response tends toward saturation.
c) In some scenarios, the dynamic range of square-law detector is simply not high enough, and the design forces the use of logarithmic envelope detector instead.

This sub-section investigates these issues by analyzing the series expansion of envelope detector profiles. The mean output signal for any envelope detector profile of the type $r_n^{(q)} = |s_n|^q$ can be calculated. Using the same method as shown in sub-sections II.B and II.C, the calculation is straight forward for even values of q, but quite cumbersome for odd q. However, it can easily be shown that for any integer q other than 2, $\mu_{r^{(q)},n}$ contains mixed terms where bits of different returns are multiplied. Therefore, for any $q \neq 2$, multiple returns would result in intermodulations.

The case of small deviation from square-law envelope detector will be modeled as an envelope detector with a response profile of 3rd order polynomial:

$$r_n' = \varepsilon_1 r_n^{(1)} + (1-\varepsilon_1-\varepsilon_3) r_n^{(2)} + \varepsilon_3 r_n^{(3)}, \tag{26}$$

where ε_1 and ε_3 are relatively small real constants.

Since the matched filter, as described in (4), is a linear and time-invariant (LTI) system, the output signal is:

$$\begin{aligned} y_n = {} & \varepsilon_1 r_n^{(1)} \otimes \tilde{c}_n \\ & + (1-\varepsilon_1-\varepsilon_3) r_n^{(2)} \otimes \tilde{c}_n \\ & + \varepsilon_3 r_n^{(3)} \otimes \tilde{c}_n. \end{aligned} \tag{27}$$

The mean value of r_n', $\mu_{r',n}$, and the mean of the normalized output signal $\mu_{y,n}$ can also be described as sums of three terms, one for each term in the series of r_n':

$$\begin{aligned} \mu_{r',n} = {} & \varepsilon_1 \mu_{r^{(1)},n} \\ & + (1-\varepsilon_1-\varepsilon_3) \mu_{r^{(2)},n} \\ & + \varepsilon_3 \mu_{r^{(3)},n}, \end{aligned} \tag{28}$$

and:

$$\begin{aligned} \mu_{y,n} = {} & \varepsilon_1 \mu_{r^{(1)},n} \otimes \tilde{c}_n \\ & + (1-\varepsilon_1-\varepsilon_3) \mu_{r^{(2)},n} \otimes \tilde{c}_n \\ & + \varepsilon_3 \mu_{r^{(3)},n} \otimes \tilde{c}_n. \end{aligned} \tag{29}$$

This notation allows us to examine the extent of sidelobes, caused by envelope detector which slightly deviates from square-law response.

For the specific case of two returns with no noise, the mean of $r_n^{(3)}$ is (due to its length, detailed derivation is not given here):

$$\begin{aligned} \mu_{r^{(3)},n} = {} & \frac{8u\sqrt{u+v}\, E\left(\frac{2v}{u+v}\right)}{3\pi} \\ & - \frac{2(u^2-v^2) K\left(\frac{2v}{u+v}\right)}{3\pi\sqrt{u+v}}, \end{aligned} \tag{30}$$

where $K(\cdot)$ and $E(\cdot)$ are the complete elliptic integral of the first and second kind, respectively [16], $u = \alpha_1^2 c_{n-d_1} + \alpha_2^2 c_{n-d_2}$ and $v = 2\alpha_1\alpha_2 c_{n-d_1} c_{n-d_2}$.

To illustrate the effect of small deviation from square profile, m-sequence is used, since as was demonstrated above for m-sequence, the intermodulation manifests as a single sidelobe. In the case of two returns with no additive noise, the mean of output signal will be of the form:

$$\mu_{y,n} = \beta_1 \delta_{n-d_1} + \beta_2 \delta_{n-d_2} + \beta_{12} \delta_{n-d_{12}}, \tag{31}$$

where β_1 and β_2 are the amplitudes of the mainlobes at delays d_1 and d_2, and β_{12} is the amplitude of the sidelobe at delay d_{12}. The delay of the sidelobe is determined by the delays of the two returns d_1 and d_2, and by the specific sequence used.

The amplitudes β_i can be computed using a property of m-sequence, where at the correct delay, '1's in the code align exactly $(N+1)/2$ times against '1's in the reference code, and at all different delays, each of the combinations '1'-'1', '0'-'1' and '1'-'0' occur $(N+1)/4$ times (this property is general for all complete Hadamard difference set (CHDS) sequence) [17]. Therefore, combining (13), (23) and (30) into (6) at $n = d_1$ gives the parameter β_1 in (31):

$$\begin{aligned} \beta_1 &= \varepsilon_1 \beta_1^{(1)} + (1-\varepsilon_1-\varepsilon_3)\beta_1^{(2)} + \varepsilon_3 \beta_1^{(3)} \\ \beta_1^{(1)} &= \frac{N+1}{4} \\ &\cdot \left[\alpha_1 - \alpha_2 + \frac{2}{\pi}(\alpha_1+\alpha_2)\, E(\tilde{u})\right] \\ \beta_1^{(2)} &= \frac{N+1}{2}\alpha_1^2 \\ \beta_1^{(3)} &= \frac{N+1}{4} \cdot \\ &\cdot \left[\begin{array}{c} \alpha_1^3 - \alpha_2^3 + \\ \frac{8(\alpha_1^2+\alpha_2^2)(\alpha_1+\alpha_2)\, E(\tilde{u})}{3\pi} - \\ \frac{2(\alpha_1-\alpha_2)^2(\alpha_1+\alpha_2) K(\tilde{u})}{3\pi} \end{array}\right], \end{aligned} \tag{32}$$

where $\tilde{u} = \frac{4\alpha_1\alpha_2}{(\alpha_1+\alpha_2)^2}$. Due to symmetry in the roles of α_1 and α_2, the parameter β_2 can be derived from (32) by switching $\alpha_1 \leftrightarrow \alpha_2$.

To calculate β_{12}, a property of m-sequence, where a modulo-2 sum of two phases of a sequence is resulted in a third phase of the sequence, yielding:

$$\begin{aligned} \beta_{12} &= \varepsilon_1 \beta_{12}^{(1)} + (1-\varepsilon_1-\varepsilon_3)\beta_{12}^{(2)} + \varepsilon_3 \beta_{12}^{(3)} \\ \beta_{12}^{(1)} &= \frac{N+1}{4}(\gamma_1+\gamma_2-\gamma_{12}) \\ &= \frac{N+1}{4} \cdot \\ &\cdot \left[\alpha_1 + \alpha_2 - \frac{2}{\pi}(\alpha_1+\alpha_2)\, E(\tilde{u})\right] \\ \beta_{12}^{(2)} &= 0 \\ \beta_{12}^{(3)} &= \frac{N+1}{4} \cdot \\ &\cdot \left[\begin{array}{c} \alpha_1^3 + \alpha_2^3 - \frac{8(a_1^2+a_2^2)(a_1+a_2)\, E(\tilde{u})}{3\pi} \\ + \frac{2(a_1-a_2)^2(a_1+a_2) K(\tilde{u})}{3\pi} \end{array}\right]. \end{aligned} \tag{33}$$

Using (31), (32) and (33), it is possible to compute the magnitude of sidelobe for this case (m-sequence with two returns). Fig. 2 shows the amplitude of ghost sidelobe $|\beta_{12}|$, relatively to the amplitude of the first target's mainlobe (β_1) in dB. The deviation from squared profile of the envelope detector is modeled by addition of small linear term (solid line) and by addition of small cubic term (dashed line). Fig. 2 (a) examines the case of two targets with equal amplitudes ($\alpha_1 = \alpha_2$), where for $\epsilon = 0.01$, the sidelobe is $-24.4dB$ and $-22dB$ bellow the mainlobe for the cases of linear and cubic deformations, respectively. As seen in Fig 2 (b), the effect becomes more significant as the amplitude of returns differ. Here, the amplitude of first return is 10 times smaller than the amplitude of the second return, and the relative sidelobe levels are $-15.7dB$ and $-19.7dB$ for the cases of linear and cubic deformations, respectively.

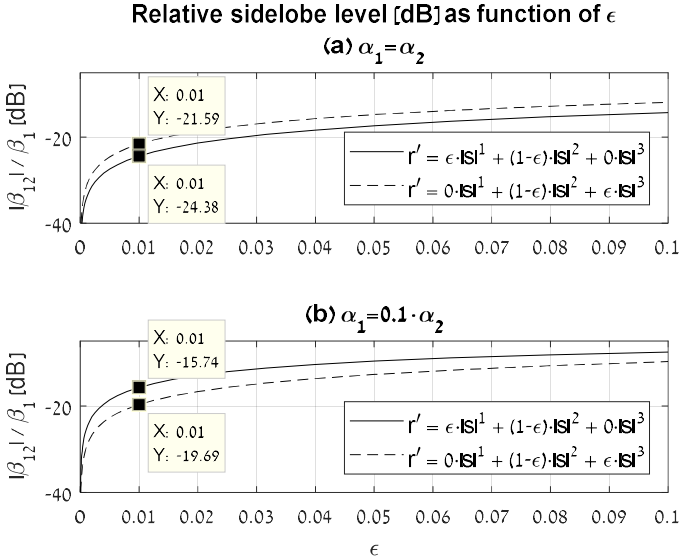

Fig. 2. Relative sidelobe level when response of envelope detector deviates from squared profile. (a) – two returns with equal amplitude ($\alpha_1 = \alpha_2$), (b) – amplitude of one return is smaller than the amplitude of the second ($\alpha_1 = \alpha_2/10$).

From (31), (32) and (33), it can be shown that as the gap in amplitude increases (return of one return is significantly stronger then other's), the sidelobe level becomes closer to the mainlobe of the lower-amplitude return.

III. Squared Envelope Calibration

As previous section showed, NCPC is sensitive to the response profile of the envelope detector, and deviations from squared response introduce intermodulations. Calibration of the envelope detector's response can solve this problem. The process of calibration can be performed either by direct or indirect measurements of the response $r_n = f(|s_n|)$.

The direct measurement can be simply performed, for example, by inserting a signal with known varying amplitude, and measuring the amplitude of the envelope-detected signal. The indirect measurement can be performed by measuring the matched filter response from scenario of **known** sets of returns (e.g. generated in an optic delay line, or a controlled test where returns can be turned on and off), and using equations (1), (2), (6), and (7), where the parameters of the inserted signal s_n (set of delays d_k and amplitudes α_k) are known. The mean values of the output signal, $\mu_{y,n}$ are measured, and the required response $f(|s_n|)$ can be computed using Least Squares (LS) estimation. Explicitly, let us model the response of the envelope detector as polynomial of order q:

$$f(|s_n|) = \sum_{l=0}^{q} \epsilon_l |s_n|^l, \tag{34}$$

where $\{\epsilon_l\}$ are $q+1$ unknown parameters, to be estimated. Note that the polynomial model is not always suitable, and for example, does not fit the cases of logarithmic detectors, or saturation. In these cases, other models should be used.

To compute the unknown parameters by LS estimation, U sets of returns are used, where for each of the set, the q moments of $|s_n|$ are calculated given the returns' amplitude and delay for each set (either analytically or numerically):

$$\mu_{r,n}^{(l,u)} = \overline{|s_{n,u}|^l}, l = 1 \dots q, u = 0 \dots U-1, \tag{35}$$

where $s_{n,u}$ is the received signal from set u of returns.

the set of linear equations to be solved is:

$$\left\{\mu_{y,n}^{(u)}\right\} = \left\{\sum_{l=0}^{q} \epsilon_l \cdot \mu_{r,n}^{(l,u)}\right\}, u = 0 \dots U-1, \tag{36}$$

and this set has a solution in an LS sense, for polynomial order smaller than the number of sets ($q+1 \le U$).

Once the response $f(|s_n|)$ is calculated, the calibration to squared-law response is performed by:

$$r_n^2 = \left(f^{-1}(r_n')\right)^2, \tag{37}$$

where $f^{-1}(\cdot)$ is the inverse of $f(\cdot)$.

To demonstrate the calibration process, a simple case of order 3 response is investigated: $r_n' = \varepsilon_1 r_n^{(1)} + \varepsilon_2 r_n^{(2)} + \varepsilon_3 r_n^{(3)}$. For the LS estimation, a model of an order 5 response will be used: $f(|s_n|) = \sum_{l=0}^{5} \epsilon_l |s_n|^l$. As the model is of order 5 polynomial, we are required to generate at least 6 unique sets of returns to estimate the response coefficients. For this example, a simple 3-returns scenario will be used: $\{\alpha_1 = 0.1, d_1 = 0\}, \{\alpha_2 = 0.5, d_2 = 10\}, \{\alpha_3 = 1, d_3 = 20\}$. $U = 7$ different sets of these 3 returns are generated, where in every set a different combination of the returns are active (the combinations are: 1st; 2nd; 3rd; 1st&2nd; 1st&3rd; 2nd&3rd; 1st&2nd&3rd). For the estimation process, $P = 1000$ periods of length $N = 127$ m-sequence are used, where for each set, the mean of the output signal $\mu_{y,n}^{(u)}$ is measured, and the moments $\mu_{r,n}^{(l,u)}$ are numerically calculated.

For this simulative demonstration, the response is set with the coefficients: $\epsilon_1 = 0.02, \epsilon_2 = 1, \epsilon_3 = 0.01$. The measured output signal, and the 5 computed moments are shown in fig. 3. Each subplot of fig. 3 presents a different set of returns. From this set of data, the estimated response is $\hat{r}_n' = \hat{\epsilon}_1 r_n^{(1)} + \hat{\epsilon}_2 r_n^{(2)} + \hat{\epsilon}_3 r_n^{(3)} + \hat{\epsilon}_4 r_n^{(4)} + \hat{\epsilon}_5 r_n^{(5)}$, where the estimated coefficients are: $\hat{\epsilon}_1 = 0.0261$, $\hat{\epsilon}_2 = 1.0049$, $\hat{\epsilon}_3 = 0.0099$, $\hat{\epsilon}_4 = -0.0031, \hat{\epsilon}_5 = 0.0002$, which fits the simulated model.

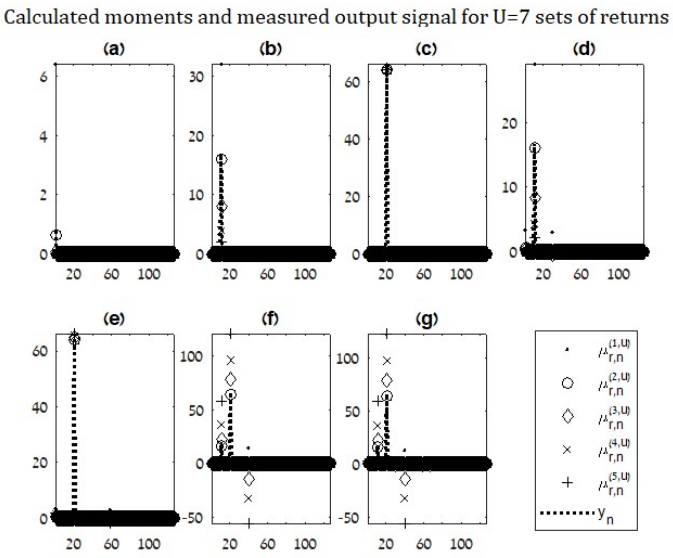

Fig. 3. Calculated moments $\mu_{r,n}^{(l,u)}$ and measured output signal y_n, for the 7 different sets of returns, where in each subplot, the active returns are: (a) α_1, (b) α_2, (c) α_3, (d) $\alpha_1\&\alpha_2$, (e) $\alpha_1\&\alpha_2$, (f) $\alpha_2\&\alpha_3$, (g) $\alpha_1\&\alpha_2\&\alpha_3$. The signal for the simulation is $P = 1000$ periods of length $N = 127$ m-sequence.

IV. Conclusion

Non-coherent pulse compression (NCPC) suffers from intermodulations as returns from multiple targets overlap. The nature of the intermodulation depends on the transmitted waveform (code length and code type), the targets (number of targets, relative delays and relative amplitudes), and the envelope detector's response profile. Using square-law envelope detector eliminates the effect of intermodulation, but it will appear if the detector deviates from squared-law profile, even slightly, therefore, the envelope detector must be calibrated to square-law response.

References

[1] M. A. Richards, *Fundamentals of Radar Signal Processing*. McGraw-Hill Education, 2005.

[2] N. Levanon and E. Mozeson, *Radar Signals*. Wiley, 2004.

[3] N. Levanon, "Noncoherent pulse compression," *IEEE Trans. Aerosp. Electron. Syst.*, vol. 42, no. 2, pp. 756–765, 2006.

[4] U. Peer and N. Levanon, "Compression Waveforms for Non-Coherent Radar," in *2007 IEEE Radar Conference*, 2007, pp. 104–109.

[5] N. Levanon, "Noncoherent Radar Pulse Compression Based on Complementary Sequences," *IEEE Trans. Aerosp. Electron. Syst.*, vol. 45, no. 2, pp. 742–747, 2009.

[6] A. Seleym, "A new non-coherent pulse compression based on binary codes for on-off keying (NCPC-BC-OOK)," in *2013 IEEE 20th International Conference on Electronics, Circuits, and Systems (ICECS)*, 2013, pp. 731–734.

[7] N. Levanon, I. Cohen, N. Arbel, and A. Zadok, "Non-coherent pulse compression — aperiodic and periodic waveforms," *IET Radar Sonar Navig.*, vol. 10, no. 1, pp. 216-224(8), Jan. 2016.

[8] M. J. Lindenfeld, "Mismatched Filters for Incoherent Pulse Compression in Laser Radar," *IEEE Trans. Aerosp. Electron. Syst.*, vol. 57, no. 2, pp. 1252–1260, 2021.

[9] E. Ben-Yaacov, D. Quartler, and N. Levanon, "Inter-pulse coding and coherent-on-receive modifications of magnetron-based marine radar – experimental results," in *2011 IEEE International Conference on Microwaves, Communications, Antennas and Electronic Systems (COMCAS 2011)*, 2011, pp. 1–9.

[10] N. Levanon, E. Ben-Yaacov, and D. Quartler, "Novel waveform for magnetron radar," in *IET International Conference on Radar Systems (Radar 2012)*, 2012, pp. 1–6.

[11] D. Kravitz, D. Grodensky, N. Levanon, and A. Zadok, "High-Resolution Low-Sidelobe Laser Ranging Based on Incoherent Pulse Compression," *IEEE Photonics Technol. Lett.*, vol. 24, no. 23, pp. 2119–2121, 2012.

[12] D. Kravitz, D. Grodensky, A. Zadok, and N. Levanon, "Incoherent compression of complementary code pairs for laser ranging and detection," in *2013 IEEE International Conference on Microwaves, Communications, Antennas and Electronic Systems (COMCAS 2013)*, 2013, pp. 1–5.

[13] N. Arbel, L. Hirschbrand, S. Weiss, N. Levanon, and A. Zadok, "Continuous-wave laser range finder based on incoherent compression of periodic sequences," in *2015 Conference on Lasers and Electro-Optics (CLEO)*, 2015, pp. 1–2.

[14] J. K. Kayani, "Performance Analysis of Noncoherent Pulse Compression Technique," *IEEE Trans. Aerosp. Electron. Syst.*, vol. 47, no. 4, pp. 2986–2990, 2011.

[15] N. Arbel, L. Hirschbrand, S. Weiss, N. Levanon, and A. Zadok, "Continuously Operating Laser Range Finder Based on Incoherent Pulse Compression: Noise Analysis and Experiment," *IEEE Photonics J.*, vol. 8, no. 2, pp. 1–11, 2016.

[16] A. Jeffrey and D. Zwillinger, *Table of Integrals, Series, and Products*. Elsevier Science, 2000.

[17] S. W. Golomb, *Shift register sequences*. Holden-Day, 1967.